Second-order error propagation in the Mueller matrix of a spectropolarimeter

I. Ilyin⋆

Leibniz-Institut für Astrophysik Potsdam (AIP), An der Sternwarte 16, D-14482 Potsdam, Germany

Received 2012 Feb 16, accepted 2012
Published online 2012

Key words stars: magnetic fields – instrumentation: spectrographs – instrumentation: polarimeters – techniques: polarimetric

Accurate measurements of Stokes IQUV in spectral lines is required for precise reconstruction of stellar magnetic field geometries with Zeeman-Dopper imaging. Spectral Zeeman features are intrinsically weak and subjected to a number of instrumental uncertainties. The aim of this work is to study the details of the instrumental uncertainties in the Stokes IQUV measurements in spectral lines and ways of their reduction. We make a practical comparison of the polarimetric performances of two high-resolution échelle spectropolarimeters, namely SOFIN at the NOT, and HARPS at ESO. We show the residual spectra for both instruments to characterize the cross-talk between the observed Stokes parameters. We employ a self-calibrating least-squares fit to eliminate some of the polarization uncertainties to derive the full Stokes vector from stellar spectra.

1 Introduction

Spectropolarimetry is a tool to measure the polarization state of the emitted light versus wavelength. As a relatively novel area in astronomy, it was mainly confined in the past to measure the Zeeman splitting in spectral lines versus rotational phase of the star in order to estimate the mean longitudinal magnetic field and infer the distribution of the multipole magnetic field (e.g. Mathys 1989).

With the advent of the Zeeman-Doppler Imaging technique (Donati & Brown 1997; Piskunov & Kochukhov 2002; Carroll et al. 2007) and its first applications to magnetic Ap and late-type stars it became possible to spatially resolve a complex structure of the stellar magnetic field distribution and its association with the surface elements of these stars. This opened up new ways in interpretation and characterization of the origin of the stellar magnetic fields and its role in stellar activity and evolution.

Recent instrumentation developments resulted in deployment of new high-resolution spectropolarimeters attached to different telescopes but of the same 3.6 m in size: ESPaDOnS at CFHT (Donati et al. 2006), SARG at TNG (Leone et al. 2003), and HARPS at ESO (Snik et al. 2011). Due to the moderate size of these telescopes, their measurements are mainly bound to Stokes V due to photon noise. The currently developed instruments are for larger telescopes and include the PEPSI spectropolarimeter (Strassmeier et al. 2008; Ilyin et al. 2011) at the 2×8.4 m Large Binocular Telescope, and a spectropolarimeter for the 39 m ESO European Extremely Large Telescope (Kochukhov & Piskunov 2008; Strassmeier 2011) which would allow solar-class ultra-high accuracy in measurements of Stokes parameters in spectral lines in terms of photon noise and spectral resolution.

The aim of this paper is to elaborate in detail the uncertainties associated with the measurements of the Stokes parameters with a polarimeter consisting of a retarder and polarizing beam-splitter. A number of papers were already dedicated to this subject with application to imaging and spectroscopic polarimeters (e.g. Eversberg et al. 1998; Keller 2002; del Toro Iniesta 2005; Patat & Romaniello 2006; Bagnulo et al. 2009; Clarke 2010). In this work though, we mainly concentrate on the description of the cross-talk between Stokes parameters due to differential transmission in the polarized beam-splitter (specifically a Foster prism), as well as due to deviations in the angles of the polarization optical elements. External effects also cause an increase of instrumental polarization, e.g. seeing, telescope and focal fore-optics or spectrograph wavelength stability but are beyond our considerations here (e.g. detailed in Clarke 2010, p. 127).

The paper is organized as follows. In Sect. 2 we briefly outline the Mueller matrices for the polarization elements we use in the subsequent Sect. 3 where we combine the results and derive the polarization modulation function. We show in Sect. 3.3 how the differential transmission of a Foster prism results in the cross-talk between Stokes I and QUV. By using Taylor series expansion up to second degree of the modulation function versus polarization elements angles in Sect. 4, we concentrate on three polarimetric configurations (no retarder, half-wave and quarter-wave retarder). In Sect. 5 we discuss various polarimetric calibration procedures and the way they applied. In Sect. 6 we eval-

⋆ Corresponding author: ilyin@aip.de

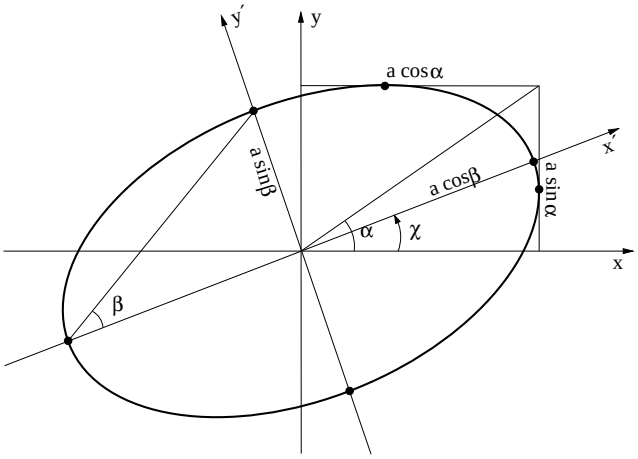

Fig. 1 An elliptically polarized monochromatic and coherent wave is propagating along axis z vertically from the picture plane (from the light source to the observer) in a right-hand Cartesian 3D coordinate system. The projection of the wave to the xy-plane makes an ellipse. The x-axis is oriented along the great circle passing through the light source and the North celestial pole.

uate the double-ratio method in terms of the above considerations. Finally, we use polarimetric spectra from the SOFIN (after a brief introduction) and HARPS spectrographs to show the residual terms of the polarimetric data reduction.

2 Preliminaries

2.1 Stokes vector of polarized light

A monochromatic and coherent electromagnetic plane wave can be described (Born & Wolf 2002, p. 25) as a composition of the following projections in a right-hand Cartesian coordinate system:

$$\begin{cases} E_x = a_x \cos(\omega t + \delta_x) \\ E_y = a_y \cos(\omega t + \delta_y) \\ E_z = 0, \end{cases} \tag{1}$$

which defines the amplitudes E_x, E_y and E_z along each axis versus time t for the given wave amplitudes a_x and a_y, angular frequency ω, and the wave phases δ_x and δ_y. The resulting vector (E_x, E_y) follows, in general, to an ellipse in the xy-plane whose major axis spans the angle χ with the axis x.

The angle χ is called the polarization (or azimuthal) angle (Fig. 1) and is counted anticlockwise in the direction *opposite* to the wave propagation axis z, i.e. as viewed from the observer towards the light source (Born & Wolf 2002, p. 29). It is conventional to orient axis x along an invariant direction, e.g., the great circle passing through the light source and the North celestial pole along the declination axis in the equatorial coordinate system (a detailed discussion of this subject is given in Clarke 2010, p. 71). The polarization angle is defined in the range $0 \le \chi \le \pi$.

The phase difference $\delta = \delta_y - \delta_x$ results in the rotation of the end of the electric vector: in case $0 < \delta < \pi$ the rotation is clockwise as the wave propagates from the light source to the observer and is called *right-hand* polarization. In case $-\pi < \delta < 0$ the rotation is anticlockwise and is called the *left-hand* polarization.

The ellipticity angle β of the polarization ellipse equals to the ratio of the electric vector amplitudes along the minor and major axes. Naturally, it varies from 0 in the case of linearly polarized light up to $\pm\pi/4$ for circularly polarized light.

The polarization radiation can be conveniently written in terms of the Stokes parameters (e.g. Born & Wolf 2002, p. 31 and Chandrasekhar 1950). A vector $\boldsymbol{s}$, which characterizes the wave amplitudes (a_x, a_y) and the phase shift δ, as well as the parameters of the polarization ellipse in terms of the total wave intensity a, ellipticity β, and the orientation angle χ is then given as:

$$\boldsymbol{s} = \begin{pmatrix} I \\ Q \\ U \\ V \end{pmatrix} = \begin{pmatrix} a_x^2 + a_y^2 \\ a_x^2 - a_y^2 \\ 2a_x a_y \cos\delta \\ 2a_x a_y \sin\delta \end{pmatrix} = \begin{pmatrix} a^2 \\ a^2 \cos 2\beta \cos 2\chi \\ a^2 \cos 2\beta \sin 2\chi \\ a^2 \sin 2\beta \end{pmatrix}. \tag{2}$$

It is useful to note that for polarized light the squared sum of the last three independent Stokes parameters,

$$I^2 = Q^2 + U^2 + V^2, \tag{3}$$

is the total intensity of the light I, whereas Q is the intensity difference between the horizontal a_x^2 and the vertical a_y^2 components of the polarized light, and U is the same but with the coordinate system turned by $\pi/4$, and V describes the direction of the rotation of the electric vector.

- The linearly polarized light is characterized by the two components E_x and E_y which are always in phase ($\delta = 0$) but each of them have different amplitudes a_x and a_y.
- The right-hand circularly polarized light occurs when the two components have the phase shift $\delta = +\pi/2$ and equal intensities while the left-hand circular polarization has $\delta = -\pi/2$.
- A constant phase shift and non-equal amplitudes result in elliptically polarized light.
- Random phase shifts and amplitudes result in unpolarized light with $Q = U = V = 0$ as the result of averaging in time, except for the total intensity $I \neq 0$.
- Weakly polarized light results in a random distribution around some value of phase shifts and amplitudes. The total intensity is in inequality $I^2 \ge Q^2 + U^2 + V^2$.

The ellipticity angle, the polarization (azimuthal) axis, and the phase difference are given as:

$$\tan 2\beta = \frac{V}{\sqrt{Q^2 + U^2}}, \quad \tan 2\chi = \frac{U}{Q}, \quad \tan\delta = \frac{V}{U}.$$

The plane wave intensities are given by

$$a_x^2 = \frac{I+Q}{2} \qquad \text{and} \qquad a_y^2 = \frac{I-Q}{2}. \tag{4}$$

2.2 Rotation of the Stokes vector

The rotation of the xy-coordinate system anticlockwise with an angle ϕ results in the reduction of the azimuthal angle χ in the rotated coordinate system χ', i.e. by introducing $\chi' = \chi - \phi$ and substituting it into (2) we readily get the transformation of the Stokes parameters into the rotated coordinate system:

$$\boldsymbol{s}' = \boldsymbol{R}(\phi) \cdot \boldsymbol{s} \tag{5}$$

with the rotation matrix

$$\boldsymbol{R}(\phi) = \begin{pmatrix} 1 & 0 & 0 & 0 \\ 0 & \cos 2\phi & \sin 2\phi & 0 \\ 0 & -\sin 2\phi & \cos 2\phi & 0 \\ 0 & 0 & 0 & 1 \end{pmatrix}. \tag{6}$$

2.3 Phase delay of the Stokes vector

An additional phase shift τ between two components of the wave is introduced to the E_y component which then propagates slower with respect to E_x, i.e. $(\delta_y + \tau) - \delta_x = \delta + \tau$. The Stokes vector with such a phase delay is

$$\boldsymbol{s}' = \boldsymbol{S}(\tau) \cdot \boldsymbol{s} \tag{7}$$

to have the transformation matrix is obtained after expansion of (2) for the new phase difference $\delta + \tau$:

$$\boldsymbol{S}(\tau) = \begin{pmatrix} 1 & 0 & 0 & 0 \\ 0 & 1 & 0 & 0 \\ 0 & 0 & \cos\tau & -\sin\tau \\ 0 & 0 & \sin\tau & \cos\tau \end{pmatrix}. \tag{8}$$

2.4 Retarders

A number of different types of designs for the optical retardation plates and their merits are detailed in Bennett (1995), as well in many other optics textbooks (e.g. Hecht 2002). Here we are interested in the Stokes vector transformation for a retarder with the fast axis oriented on angle ϕ with respect to the reference polarization axis x. The transformation of the Stokes vector $\mathbf{s}$ involves the rotation of the Stokes vector onto the fast optic axis of the optical retarder, the phase delay, and the de-rotation of the vector back to the original coordinate system xy:

$$\boldsymbol{s}' = \boldsymbol{R}(-\phi) \cdot \boldsymbol{S}(\tau) \cdot \boldsymbol{R}(\phi) \cdot \boldsymbol{s} = \boldsymbol{A}(\phi, \tau) \cdot \boldsymbol{s}. \tag{9}$$

There the retarder matrix becomes

$$\boldsymbol{A}(\phi, \tau) = \begin{pmatrix} 1 & 0 & 0 & 0 \\ 0 & A_{22} & A_{23} & A_{24} \\ 0 & A_{32} & A_{33} & -A_{34} \\ 0 & -A_{42} & A_{43} & \cos\tau \end{pmatrix} \tag{10}$$

with the elements (e.g. similar to Collet 1993, p. 82):

$$\begin{aligned} A_{22} &= \cos^2 2\phi + \sin^2 2\phi \cos\tau \\ A_{33} &= \sin^2 2\phi + \cos^2 2\phi \cos\tau \\ A_{32} &= A_{23} = \sin 2\phi \cos 2\phi \,(1 - \cos\tau) \\ A_{42} &= A_{24} = \sin 2\phi \sin\tau \\ A_{34} &= \cos 2\phi \sin\tau. \end{aligned} \tag{11}$$

Note that for the retarder with zero phase delay $\tau = 0$ (i.e. no retarder) the polarization matrix equals to the identity matrix $\boldsymbol{A}(0, 0) = \boldsymbol{I}$. The half-wave retarder $\tau = \pi$ turns the polarization plane at angle χ to the new orientation $2\phi - \chi$ and reverses the sign of the circular polarization V. The quarter-wave retarder $\tau = \pi/2$ transforms circularly polarized light into linearly polarized light and vice verse.

2.5 Transmission of the Stokes vector

Polarizing beam splitters separate incident light into two orthogonally polarized beams. Usually, a combination of one or two uniaxial birefringent materials (e.g. calcite) with a specific orientations of the optic axes is employed. This is in order to make use of the birefringence effect for the spatial separation of the polarized beams (Bennett 1995). Each polarized beam is characterized by the maximal transmittance coefficient T_1 along its polarization plane and by the minimal transmittance coefficient T_2 for the orthogonal plane. Ideally, the transmittance coefficients T_1 and T_2 for the two emerged beams should be the same. In reality though, the emerged beams become slightly elliptically polarized, due to numerous imperfection factors in the birefringent medium or manufacturing and polishing misalignment of the optic axis (Bennett 1995, p. 3.15). Moreover, in the prisms where the total internal reflection is used to separate the beams, the effect of multiple beam interference is present in the straight-through beam resulting in a back reflection and contamination of the other beam which becomes elliptically polarized. Therefore, we shall consider separate transmission coefficients for each beam.

For an elementary plane wave with incident amplitudes a_x, a_y and axis x oriented along the optic axis of the birefringent, the transmitted amplitudes of the beam are:

$$\begin{cases} (a_x^+)^2 = T_1^+ \, a_x^2 \\ (a_y^+)^2 = T_2^+ \, a_y^2 \end{cases} \quad \text{and} \quad \begin{cases} (a_x^-)^2 = T_2^- \, a_x^2 \\ (a_y^-)^2 = T_1^- \, a_y^2. \end{cases} \tag{12}$$

The wave has a polarization plane parallel to the optic axis of the birefringent ("+" along x or e-beam) and for the other beam which has a polarization plane perpendicular to the optic axis ("−" along y or o-beam). In the case of a polarizer, the second component (a_x^-, a_y^-) is absorbed and its elements are zeroed. The resulting Stokes vectors for the two orthogonal beams are

$$\boldsymbol{s}^+ = \begin{pmatrix} T_1^+ a_x^2 + T_2^+ a_y^2 \\ T_1^+ a_x^2 - T_2^+ a_y^2 \\ 2\sqrt{T_1^+ T_2^+}\, a_x a_y \cos\delta \\ 2\sqrt{T_1^+ T_2^+}\, a_x a_y \sin\delta \end{pmatrix} \tag{13}$$

and

$$\boldsymbol{s}^- = \begin{pmatrix} T_2^- a_x^2 + T_1^- a_y^2 \\ T_2^- a_x^2 - T_1^- a_y^2 \\ 2\sqrt{T_1^- T_2^-}\, a_x a_y \cos\delta \\ 2\sqrt{T_1^- T_2^-}\, a_x a_y \sin\delta \end{pmatrix}. \tag{14}$$

Comparing it with (2), and using (4), the transformation of the Stokes vector is

$$\boldsymbol{s}^\pm = \boldsymbol{T}(T_1^\pm, T_2^\pm) \cdot \mathbf{s} \tag{15}$$

with the transmission matrix

$$\boldsymbol{T}(T_1^\pm, T_2^\pm) = \begin{pmatrix} A^\pm & \pm B^\pm & 0 & 0 \\ \pm B^\pm & A^\pm & 0 & 0 \\ 0 & 0 & C^\pm & 0 \\ 0 & 0 & 0 & C^\pm \end{pmatrix} \tag{16}$$

and the new notations

$$A^\pm = \frac{T_1^\pm + T_2^\pm}{2}, \qquad B^\pm = \frac{T_1^\pm - T_2^\pm}{2}, \qquad C^\pm = \sqrt{T_1^\pm\, T_2^\pm}. \tag{17}$$

This satisfies $A^2 = B^2 + C^2$ and the relative transmittance ratio is $F^\pm = B^\pm / A^\pm$ for each of the two beams.

2.6 Polarizing the Stokes vector

The transformation of the Stokes parameters transmitted through a rotating polarizing beam splitter can be written as a product of three matrices:

$$\boldsymbol{s}^\pm = \boldsymbol{R}(-\psi) \cdot \boldsymbol{T}(T_1^\pm, T_2^\pm) \cdot \boldsymbol{R}(\psi) \cdot \boldsymbol{s} = \boldsymbol{B}(T_1^\pm, T_2^\pm, \psi) \cdot \boldsymbol{s}, \tag{18}$$

where the angle ψ is the angle between the optic axis of the polarizing beam splitter and the reference azimuthal axis x. If the first rotation matrix $\boldsymbol{R}(\psi)$ describes the vector transformation onto the inclined principal axis of the polarizer, then the transmission matrix $\boldsymbol{T}(T_1^\pm, T_2^\pm)$ describes the change of the vector for the two transmitted beams, while the last operator de-rotates the vector back to the original (reference) coordinate system. The matrix multiplications result in (we omit $\pm$ in every A, B, and C):

$$\boldsymbol{B}(T_1^\pm, T_2^\pm, \psi) = \begin{pmatrix} A & B_{12} & B_{13} & 0 \\ B_{21} & B_{22} & B_{32} & 0 \\ B_{31} & B_{32} & B_{33} & 0 \\ 0 & 0 & 0 & C \end{pmatrix}, \tag{19}$$

with its elements

$$\begin{aligned} B_{22} &= A\cos^2 2\psi + C\,\sin^2 2\psi \\ B_{33} &= A\sin^2 2\psi + C\cos^2 2\psi \\ B_{32} &= B_{23} = (A - C)\sin 2\psi \cos 2\psi \\ B_{12} &= B_{21} = \pm B\cos 2\psi \\ B_{31} &= B_{13} = \pm B\sin 2\psi. \end{aligned} \tag{20}$$

As before, the "+" sign indicates the transmitted beam whose polarization plane is parallel to the principal (optic) axis of the birefringent, and "−" indicates the transmitted beam with the polarization plane perpendicular to the optic axis.

Turning the birefringent to $90°$ exchanges the above correspondence, i.e. $\boldsymbol{s}^\pm \rightarrow \boldsymbol{s}^\mp$. Note that $\boldsymbol{B}(T_1^\pm, T_2^\pm, 0) = \boldsymbol{T}(T_1^\pm, T_2^\pm)$.

For an ideal beam splitter with $T_1 = 1$, and $T_2 = 0$, and oriented along axis x ($\psi = 0$), the two components of the Stokes vector of the emerged light are

$$I^\pm = \frac{I \pm Q}{2}, \quad Q^\pm = \frac{\pm I + Q}{2}, \quad I^\pm = \pm Q^\pm. \tag{21}$$

3 Polarimeter with retarder and polarizing beam splitter

The real transformation of the Stokes parameters is the product of the retarder and the beam-splitter polarization matrices:

$$\boldsymbol{s}^\pm = \boldsymbol{B}(T_1^\pm, T_2^\pm, \psi) \cdot \boldsymbol{A}(\phi + \psi, \tau) \cdot \boldsymbol{s}. \tag{22}$$

Firstly note that the birefringent optic axis angle ψ is counted from the reference polarization axis x aligned to the celestial North pole. The *relative* rotation angle of the retarder ϕ is counted here with respect to the optic axis of the beam splitter.

Secondly note that the above rotation angles have to be counted in the *same* direction as the polarization angle χ is reckoned, i.e. anticlockwise in the direction from the observer to the light source.

Since the detector is only able to measure the light intensity $I^\pm$ of the resulting Stokes vector $\boldsymbol{s}^\pm$, we are interested only in the first row of the matrix (22), which gives

$$I^\pm(T_1^\pm, T_2^\pm, \psi, \phi, \tau) = A^\pm \cdot I \pm B^\pm \cdot P(\psi, \phi, \tau), \tag{23}$$

where the polarization modulation function

$$P(\psi, \phi, \tau) = Q a_0 + U a_1 + V a_2 \tag{24}$$

is the linear combination of the Stokes QUV as seen in the expanded form:

$$\begin{aligned} &P(\psi, \phi, \tau) = V \sin 2\phi \sin\tau + \\ &\Big(Q\cos(2\phi + 2\psi) + U\sin(2\phi + 2\psi)\Big)\cos 2\phi + \\ &\Big(Q\sin(2\phi + 2\psi) - U\cos(2\phi + 2\psi)\Big)\sin 2\phi \cos\tau. \end{aligned} \tag{25}$$

A similar result for retarder and polarizer used in ellipsometry is given in Landi Degl'Innocenti & Landolfi (2004, p. 19), note the opposite sign of $\phi - \psi$ and the absolute value of ϕ.

For the polarimeter with no retarder present with $\tau = \phi = 0$, the polarization modulation function becomes

$$P(\psi, 0, 0) = Q\cos 2\psi + U\sin 2\psi. \tag{26}$$

Then, for the half-wave retarder with $\tau = 180°$ we have

$$P(\psi,\phi,180) = Q\cos(4\phi{+}2\psi){+}U\sin(4\phi{+}2\psi) \tag{27}$$

and for the quarter-wave retarder with $\tau = 90°$ the last term in (25) vanishes and we have

$$\begin{aligned} P(\psi,\phi,90) &= V\sin 2\phi{+}\\ &\Big(Q\cos(2\phi+2\psi)+U\sin(2\phi+2\psi)\Big)\cos 2\phi. \end{aligned} \tag{28}$$

This can be decomposed into

$$P(\psi,\phi,90) = \frac{1}{2}\Big(P(\psi,0,0)+P(\psi,\phi,180)\Big)+V\sin 2\phi$$

as the halved sum of the two polarization modulation functions P for polarimeters with $\tau = 0$ and $\tau = 180°$, plus the circular polarization V modulation term.

3.1 Combination of normalized intensities

The intensity of the light $I^{\pm}$ from each of two polarized beams transmitted through a spectrograph and recorded on the detector is subjected to numerous multiplicative transformations (guiding, fiber transmission, attenuation on échelle, optical vignetting, detector response) described by $f^{\pm}$, so that the stellar $J^{\pm}$ and the respective continuum $J_c^{\pm}$ fluxes are recorded as

$$J^{\pm} = f^{\pm}I^{\pm} \qquad \text{and} \qquad J_c^{\pm} = f^{\pm}I_c^{\pm}. \tag{29}$$

The intensities $r^{\pm}$ normalized to un-polarized continuum ($I_c^{\pm} = A^{\pm}I_c$) become

$$\begin{aligned} r^{\pm} = \frac{J^{\pm}}{J_c^{\pm}} = \frac{I^{\pm}}{I_c^{\pm}} = \frac{A^{\pm}I \pm B^{\pm}P}{A^{\pm}I_c} = \\ \frac{I}{I_c} \pm F^{\pm}\cdot\frac{P}{I_c} = i \pm F^{\pm}p \end{aligned} \tag{30}$$

where the relative transmittance ratio is as before $F^{\pm} = B^{\pm}/A^{\pm}$. We now denote all continuum normalized Stokes intensities with *small* letters, i.e. $i = I/I_c$ and the polarization modulation function (24) becomes

$$p = \frac{P(\psi,\phi,\tau)}{I_c} = qa_0 + ua_1 + va_2. \tag{31}$$

The sum s and the difference d of the two normalized intensities are

$$\begin{cases} s = r^+ + r^- = 2\cdot i + (F^+ - F^-)\cdot p \\ d = r^+ - r^- = \qquad (F^+ + F^-)\cdot p. \end{cases} \tag{32}$$

If we denote s_1 and d_1 when the modulation function p_1 is obtained at one angle, and s_2 and d_2 for p_2 at another angle, then their combinations become:

$$\begin{cases} s_1 + s_2 = 4\cdot i + (F^+ - F^-)\cdot(p_1+p_2) \\ s_1 - s_2 = \qquad (F^+ - F^-)\cdot(p_1-p_2) \end{cases} \tag{33}$$

and

$$\begin{cases} d_1 + d_2 = (F^+ + F^-)\cdot(p_1+p_2) \\ d_1 - d_2 = (F^+ + F^-)\cdot(p_1-p_2). \end{cases} \tag{34}$$

The derived Stokes parameters q, u, or v are always scaled down by the transmission factors $F^+ + F^-$ which can be also wavelength dependent. Normalized Stokes intensity $i = I/I_c$ may have a cross-talk with the corresponding Stokes parameter if the latter are derived from the sum $p_1 + p_2$. It is useful to note that

$$\begin{cases} s_1 + s_2 = 4\cdot i + \dfrac{F^+ - F^-}{F^+ + F^-}\cdot(d_1+d_2) \\ s_1 - s_2 = \qquad \dfrac{F^+ - F^-}{F^+ + F^-}\cdot(d_1-d_2). \end{cases} \tag{35}$$

3.2 An ideal polarizing beam-splitter

In case of symmetric transmission of the two polarized beams $T_1 = T_1^{\pm}$ and $T_2 = T_2^{\pm}$, the relative transmission coefficient becomes

$$F = F^{\pm} = \frac{T_1 - T_2}{T_1 + T_2}. \tag{36}$$

In ideal case $T_2 = 0$, hence $F = 1$. The above combinations of the continuum normalized intensities from two polarized beams obtained at two angles of the polarization elements become more simplified:

$$\begin{cases} s_1 + s_2 = 4\cdot i \\ s_1 - s_2 = 0 \end{cases} \tag{37}$$

and

$$\begin{cases} d_1 + d_2 = 2\,F\cdot(p_1+p_2) \\ d_1 - d_2 = 2\,F\cdot(p_1-p_2). \end{cases} \tag{38}$$

For most of the commercially available polarizing beam-splitters designed on the principle of double refraction (e.g. calcite polarizers or Wollaston prism), the extinction ratio T_2/T_1 is of the order of 10^{-5}–10^{-6} (Bennet 1995; Halle 2011) and can be considered as the 'ideal' polarizers.

3.3 The Foster prism

The Foster prism (or more precisely the polarizing beam-splitting Glan-Thompson prism) is designed on the principle of the total internal reflection of the ordinary beam (having a larger refractive index) from the interface layer between two calcite blocks, while the extraordinary beam with the smaller refractive index is transmitted directly through the two blocks. The tricky part, though, is the refractive index matching adhesive between the two blocks to minimize the transmission losses of the extraordinary beam. Any deviations of the refractive index of the adhesive from that of the extraordinary beam results in a back reflection of the beam which then undergoes on the same optical path as the ordinary beam, so that the reflected beam becomes elliptically polarized (a phase difference is introduced due to differences in the optical paths of the two beams). Furthermore, the multiple beam interference occurs on the plane-

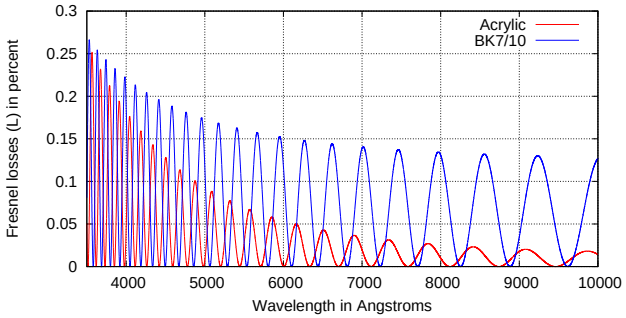

Fig. 2 (online colour at: www.an-journal.org) Fresnel losses L in percent in the Foster prism for acrylic and BK7 (scaled down by 10) adhesives on the interface between two calcite blocks with the thickness of the gap 10 μm.

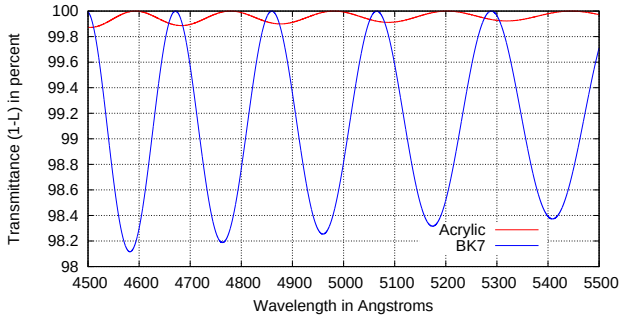

Fig. 3 (online colour at: www.an-journal.org) Fragment of the previous picture showing the shape of the transmittance profile for the two adhesives of the interface layer.

parallel interface between the calcite blocks resulting in the ripples of the transmission peaks of the extraordinary beam. The minimum of the transmission corresponds to the maximum of the back reflection and contamination of the ordinary beam at certain wavelengths. It seems to our knowledge that the effect of multiple beam interference on the beam-splitter interface layer has not been noticed or considered in the past. An effect of the similar nature of wavelength-dependent phase delay due to multiple beam interference on the retarder plate acting also as a weak polarized was described by Semel (2003) and Clarke (2005).

There are no direct measurements available of the Fresnel losses for commercial polarizing beam-splitters and it is not possible to model it because proprietary adhesives are used in most cases. There are some indications that the reflected ordinary beam is 'heavily contaminated' by the extraordinary beam (Metz 1984; Bennet 1995; Goodrich 1991; Halle 2011). The latter indicate that it may be of the order of few percent for a polarizing beam splitter.

In Ilyin et al. (2011) we present a solution for the optimal adhesive (acrylic matching liquid) and its modeling of the Fresnel transmission for a custom designed Foster prism in order to minimize the effect of beam contamination which would be of the order of 0.2–0.02% for the optical wavelength range. For any other adhesive solution with refractive index mismatch (BK7 matching liquid), the back reflection increases up to 2.5–1.5% over the optical wavelength range. The latter can be used as a proxy for proprietary adhesives used in commercially available polarizing beam-splitters. Fig. 2 shows the modeling of the Fresnel losses L modulated by the multiple beam interference (Born & Wolf 2002, p. 362) for above two types of Foster prism interfaces where the transmissions on the entrance and exit surfaces are taken into account, as well as on the additional deflection prism.

In the following, we derive the relative transmittance for the extraordinary ("+") and ordinary ("−") beams. Here we neglect the transmission losses of the two rays at the entrance and exit surfaces, the difference in absorption due to optical path lengths, and the absorption on the interface layers of the calcite and deflection prisms. The straight-through extraordinary beam, $T_1^+ = 1 - L$, of the incident intensity is transmitted along the reference polarization axis x oriented along the optic axis of the calcite prism and nothing is added $T_2^+ = 0$ along axis y (again neglecting calcite prism manufacturing imperfections with the extinction ratio of the order of 10^{-6}, Bennet 1995, p. 3.15). For the ordinary beam with the total internal reflection at the interface layer, the maximal transmission along axis y is $T_1^- = 1$, and the residual intensity $T_2^- = L$ along axis x comes from the multiple beam interference of the extraordinary beam:

$$\begin{cases} T_1^+ = 1 - L \\ T_2^+ = 0 \end{cases} \qquad \begin{cases} T_2^- = L \\ T_1^- = 1. \end{cases} \tag{39}$$

The sum and the difference of the relative transmittances for two polarized beams become

$$\begin{cases} F^+ + F^- = \dfrac{2}{1+L} \simeq 2\,(1-L) \\ F^+ - F^- = \dfrac{2L}{1+L} \simeq 2\,L. \end{cases} \tag{40}$$

The sum and the difference of the two continuum normalized intensities are

$$\begin{cases} s = r^+ + r^- = 2 \cdot i + \dfrac{2L}{1+L} \cdot p \\ d = r^+ - r^- = \dfrac{2}{1+L} \cdot p, \end{cases} \tag{41}$$

i.e. the normalized intensity profile is always contaminated by a small fraction of the polarization profile Stokes Q, U, or V. The combination of sums s_1 and s_2, and differences d_1 and d_2 of the continuum normalized intensities of the

two polarized beams obtained at two different angles of the polarization elements (e.g. retarder) are:

$$\begin{cases} s_1 + s_2 = 4 \cdot i + \dfrac{2L}{1+L} \cdot (p_1 + p_2) \\ s_1 - s_2 = \qquad \dfrac{2L}{1+L} \cdot (p_1 - p_2) \end{cases} \tag{42}$$

and

$$\begin{cases} d_1 + d_2 = \dfrac{2}{1+L} \cdot (p_1 + p_2) \\ d_1 - d_2 = \dfrac{2}{1+L} \cdot (p_1 - p_2). \end{cases} \tag{43}$$

Note that for the Foster prism we have

$$s_1 - s_2 = L \cdot (d_1 - d_2). \tag{44}$$

3.3.1 Polarization interference on the interface layer

The optical interference on the interface layer has little or second order effect on the normalized Stokes i intensity profile if the sum of the polarization modulation function at two angles $p_1 + p_2$ is small (42). On the other hand, it causes modulation (43) of the derived Stokes QUV parameters by the value of $1 - L$ versus wavelength as shown in Fig. 3 for the interface layer thickness of $10\,\mu$m. The larger the thickness, the shorter the distance between the interference fringes.

The free spectral range of the optical interference on a layer with thickness h with refractive index n at wavelength λ and incident angle θ is

$$\Delta\lambda_{\rm FSR} = \frac{\lambda^2}{2nh\cos\theta}. \tag{45}$$

The free spectral range of the échelle spectrograph at the blaze wavelength λ of the spectral order k is

$$\Delta\Lambda_{\rm FSR} \simeq \frac{\Lambda_1}{k^2} \tag{46}$$

where $\Lambda_1 = k\lambda$ is the blaze wavelength of the first spectral order. The distance between the interference fringes is equal to the length of spectral orders ($\Delta\lambda_{\rm FSR} = \Delta\Lambda_{\rm FSR}$) if the thickness is

$$h = \frac{\Lambda_1}{2n\cos\theta}. \tag{47}$$

For an R4 échelle grating with 31.6 grooves/mm we have $\Lambda_1 = 61.4\,\mu$m (the case of PEPSI (Strassmeier 2008) and HARPS (Snik 2011) spectropolarimeters), the refractive index $n = 1.5$, and for the incidence angle $90^\circ - \alpha = 67.5^\circ$ (where $\alpha = 22.5^\circ$ is the apex angle of the Foster prism), the thickness of the adhesive layer is $h = 53\,\mu$m. Thus, for a typical thickness of the interface layer of $10\,\mu$m, the interval between successive maxima is spanning over five échelle orders.

Since the reflectivity on the interface layer is rather small, the reflective finesse, defined as the ratio of the distance between successive peaks and the FWHM of the peaks (at 50% transmittance), is less than one, i.e. the transmission peaks are heavily overlapped and have a shape of the cosine function (Born & Wolf 2002, p. 364).

4 Error propagation in the polarization vector

As for now, we considered the effect of finite transmissions in the polarizing beam-splitter on the cross-talk between Stokes I and QUV. Here we are considering the effect of misalignment and deviation of the angles of the polarization elements which may result in the mutual cross-talk between Stokes Q, U and V.

The polarization modulation function $P(\psi, \phi, \tau)$ in (25) depends on ψ being the orientation of the polarizing beam-splitter optic axis along the reference azimuthal axis x, ϕ as the orientation of the fast axis of the retarder with respect to the optic axis of the beam-splitter, and τ as the phase delay angle of the retarder. In the Taylor expansion of the function over its three angles we retain here the following terms:

$$\begin{aligned} P(\psi + \Delta\psi, \phi + \Delta\phi, \tau + \Delta\tau) = P(\psi, \phi, \tau) + \\ \frac{\partial P}{\partial \phi} \cdot \Delta\phi + \frac{\partial^2 P}{\partial \phi^2} \cdot \frac{\Delta\phi^2}{2} + \frac{\partial P}{\partial \tau} \cdot \Delta\tau + \\ \frac{\partial^2 P}{\partial \tau^2} \cdot \frac{\Delta\tau^2}{2} + \frac{\partial^2 P}{\partial \phi\, \partial \tau} \cdot \Delta\phi\Delta\tau + \frac{\partial P}{\partial \psi} \cdot \Delta\psi. \end{aligned} \tag{48}$$

By using this expansion, we analyze in the following the error propagation in the polarization modulation function and its effect on the derived Stokes parameters as a function of deviations in polarization element angles for three different configuration of polarimeters: with no retarder, and with half and quarter-wave retarders. The deviation in the angles are mostly due to wavelength dependent chromatic effects in retardation angle of the retarder, change in orientation of its fast axis with wavelength or misalignment, and misalignment of the optic axis of the beam-splitter with respect to the reference polarization axis.

4.1 A polarimeter with polarizing beam-splitter and no retarder

For a polarimeter with no retarder, i.e. $\tau = \phi = 0$, the polarization modulation function (26) for the beam-splitter has the simplest form:

$$P(\psi, 0, 0) = Q\cos 2\psi + U\sin 2\psi \tag{49}$$

so that

$$\begin{cases} P_0 = \quad -P_{90} = \quad Q + U \cdot 2\Delta\psi \\ P_{45} = \; -P_{135} = \; U - Q \cdot 2\Delta\psi, \end{cases} \tag{50}$$

i.e. Q and U are known up to the uncertainty in the beam-splitter orientation angle $\Delta\psi$. The Stokes Q or U can be obtained just in two exposures if the relative transmission

difference $F^+ - F^-$ in (32) is small and the cross-talk between Stokes I and Q or U can be neglected. Otherwise a combination of two angles separated by 90° must be used:

$$\begin{cases} P_0 + P_{90} = P_{45} + P_{135} = 0 \\ P_0 - P_{90} = 2\,(Q + U \cdot 2\Delta\psi) \\ P_{45} - P_{135} = 2\,(U - Q \cdot 2\Delta\psi) \end{cases} \quad (51)$$

which results in the combinations of sums s and differences d of the continuum normalized intensities of the two polarized beams obtained at the two angles:

$$\begin{cases} s_0 + s_{90} & = s_{45} + s_{135} = 4 \cdot i \\ s_0 - s_{90} & = 2\,(F^+ - F^-) \cdot (q + u \cdot 2\Delta\psi) \\ s_{45} - s_{135} & = 2\,(F^+ - F^-) \cdot (u - q \cdot 2\Delta\psi) \end{cases} \quad (52)$$

and

$$\begin{cases} d_0 + d_{90} & = d_{45} + d_{135} = 0 \\ d_0 - d_{90} & = 2\,(F^+ + F^-) \cdot (q + u \cdot 2\Delta\psi) \\ d_{45} - d_{135} & = 2\,(F^+ + F^-) \cdot (u - q \cdot 2\Delta\psi). \end{cases} \quad (53)$$

The first line in (52) gives continuum-normalized Stokes I free of cross-talk and the last two lines in (53) give continuum-normalized Q and U scaled by the relative transmission factors. The other lines are given for completeness.

4.2 A polarimeter with half-wave retarder and polarizing beam-splitter

A polarimeter with a half-wave retarder $\tau = 180^\circ$ in front of the polarizing beam-splitter allows to measure only linearly polarized light. Its polarization modulation function (27) is

$$P(\psi, \phi, 180) = Q\cos(4\phi + 2\psi) + U\sin(4\phi + 2\psi). \quad (54)$$

Although the function P is periodic with $\phi = 90^\circ$, the terms in the error expansion (48) are not. Useful to note that the rotation of the beam-splitter by $\pm 90^\circ$ results in the sign reverse of the Stokes Q and U: $P(\psi \pm 90, \phi, 180) = -P(\psi, \phi, 180)$. From (4) we derive computer-generated combinations of the modulation function for two different angles of the half-wave retarder ϕ and these are given in (55) where all multiples for Q, U, and V are combined in three columns. The first part of the table determines Stokes Q and the second part Stokes U.

The combination of two angles of the half-wave retarder separated by 45°, $(P_0 - P_{45})$ and $(P_{45} - P_{90})$ determines Stokes Q co-added with its linear cross-talk term $\Delta\phi$ over U and the term $\Delta\tau$ over V. The contamination of Q by V can not be negligible in the case of non-zero retardation error $\Delta\tau$ and strong Stokes V which can be of order of a magnitude larger than Q. For the retardation error of, e.g., $1^\circ \simeq 2\%$, the Stokes Q profile is contaminated by 1% of V, and in case $V = 10 \times Q$ at a specific wavelength of the line profile, the value of Q will be distorted by 10% of its own amplitude.

It should be noted that if we co-add $(P_0 - P_{45})$ and $(P_0 + P_{45})$, then the cross-talk term $\Delta\tau$ in V for P_0 vanishes, i.e. it comes solely from the second angle P_{45}. The difference of these two angles, aimed to cancel out the residual terms, does not work in this case and introduces additional cross-talk terms instead.

The other combination of the retarder angles separated by 90°, $(P_0 + P_{90})$ and $(P_{45} + P_{135})$, have similar error budget in U, but no cross-talk with V at all. However, this benefit has two disadvantages: firstly, the sum of two continuum normalized intensities is sensitive to small errors of the continuum fit (opposite to the intensity difference when these misfits can mutually be canceled out) and, secondly as before, has cross-talk between Stokes I and Q when the relative transmission difference $F^+ - F^-$ of the beam-splitter in (32) is not negligible (i.e. for the 1% case, the normalized Stokes i is contaminated by 1% of q).

The error budget in Stokes U at the second half of the table is rather similar to that of the Q: the two combinations of the retarder angles separated by 45° have a linear cross-talk term $\Delta\phi$ over Q, a linear term $\Delta\tau$ over V for $(P_{67.5} - P_{112.5})$, and the negligible quadratic term $\Delta\phi\Delta\tau$ over V for $(P_{22.5} - P_{67.5})$.

As before, the combination with an angle separation by 90°, $(P_{22.5} + P_{112.5})$ and $(P_{67.5} + P_{157.5})$, has no residual cross-talk in V, but as the sum of normalized intensities has the same potential disadvantages as discussed in the case of Q.

All residual combinations of two angles we shall call the *residual spectrum* as it reflects the amplitude of the deviations in the angles of the polarization elements. The combination, e.g. $(P_{45} - P_{135})$, is the scaled down replica of Stokes V by a factor $\Delta\tau$.

It is worth to mention that any other combinations of angles, like separated by 30° in order to obtain Q and U only in three exposures, would lead to a heavily contaminated series of un-reducible residuals.

4.3 A polarimeter with quarter-wave retarder and polarizing beam-splitter

For the quarter-wave retarder with $\tau = 90^\circ$ the polarization modulation function is given in (28). Similarly to the previous section, we derive combinations of the modulation function for two different angles of the quarter-wave retarder ϕ which are given in (56) where all multiples for Q, U, and V are combined in three columns.

The combination of two angles $(P_{45} - P_{135})$ is ideal to determine Stokes V since it retains only second order terms in V and first order terms in Q and U. The sum $(P_0 + P_{90})$ determines Stokes Q but retains the first order terms in U. For the combinations of angles separated by 45°, we have

$$\sqrt{2}\,(P_{45} - P_{135}) = (P_{22.5} - P_{112.5}) + (P_{67.5} - P_{157.5}),$$

$P_1 \pm P_2$	$2Q$	$2U$	$2V$
$P_0 - P_{45}$	$+1 - 8 \cdot \Delta\phi^2 - 0.25 \cdot \Delta\tau^2$	$+4 \cdot \Delta\phi + 2 \cdot \Delta\psi$	$+0.5 \cdot \Delta\tau - \Delta\phi\Delta\tau$
$P_0 + P_{45}$	$+0.25 \cdot \Delta\tau^2$		$-0.5 \cdot \Delta\tau - \Delta\phi\Delta\tau$
$P_{45} - P_{90}$	$-1 + 8 \cdot \Delta\phi^2 + 0.25 \cdot \Delta\tau^2$	$-4 \cdot \Delta\phi - 2 \cdot \Delta\psi$	$-0.5 \cdot \Delta\tau - \Delta\phi\Delta\tau$
$P_{45} + P_{90}$	$+0.25 \cdot \Delta\tau^2$		$-0.5 \cdot \Delta\tau + \Delta\phi\Delta\tau$
$P_0 - P_{90}$			$-2 \cdot \Delta\phi\Delta\tau$
$P_0 + P_{90}$	$+1 - 8 \cdot \Delta\phi^2$	$+4 \cdot \Delta\phi + 2 \cdot \Delta\psi$	
$P_{45} - P_{135}$			$-\Delta\tau$
$P_{45} + P_{135}$	$-1 + 8 \cdot \Delta\phi^2 + 0.5 \cdot \Delta\tau^2$	$-4 \cdot \Delta\phi - 2 \cdot \Delta\psi$	
$P_{22.5} - P_{67.5}$	$-4 \cdot \Delta\phi - 2 \cdot \Delta\psi$	$+1 - 8 \cdot \Delta\phi^2 - 0.25 \cdot \Delta\tau^2$	$-\sqrt{2} \cdot \Delta\phi\Delta\tau$
$P_{22.5} + P_{67.5}$	$+0.25 \cdot \Delta\tau^2$		$-\sqrt{2}/2 \cdot \Delta\tau$
$P_{67.5} - P_{112.5}$	$+4 \cdot \Delta\phi + 2 \cdot \Delta\psi$	$-1 + 8 \cdot \Delta\phi^2 + 0.25 \cdot \Delta\tau^2$	$-\sqrt{2}/2 \cdot \Delta\tau$
$P_{67.5} + P_{112.5}$	$+0.25 \cdot \Delta\tau^2$		$+\sqrt{2} \cdot \Delta\phi\Delta\tau$
$P_{22.5} - P_{112.5}$			$\sqrt{2} \cdot (-0.5 \cdot \Delta\tau - \Delta\phi\Delta\tau)$
$P_{22.5} + P_{112.5}$	$-4 \cdot \Delta\phi + 0.25 \cdot \Delta\tau^2 - 2 \cdot \Delta\psi$	$+1 - 8 \cdot \Delta\phi^2 - 0.25 \cdot \Delta\tau^2$	
$P_{67.5} - P_{157.5}$			$\sqrt{2} \cdot (-0.5 \cdot \Delta\tau + \Delta\phi\Delta\tau)$
$P_{67.5} + P_{157.5}$	$+4 \cdot \Delta\phi + 0.25 \cdot \Delta\tau^2 + 2 \cdot \Delta\psi$	$-1 + 8 \cdot \Delta\phi^2 + 0.25 \cdot \Delta\tau^2$	

(55)

$P_1 \pm P_2$	$2Q$	$2U$	$2V$
$P_0 - P_{90}$			$+2 \cdot \Delta\phi$
$P_0 + P_{90}$	$+1 - 4 \cdot \Delta\phi^2$	$+2 \cdot \Delta\phi + 2 \cdot \Delta\phi\Delta\tau + 2 \cdot \Delta\psi$	
$P_{45} - P_{135}$			$+1 - 2 \cdot \Delta\phi^2 - 0.5 \cdot \Delta\tau^2$
$P_{45} + P_{135}$	$+4 \cdot \Delta\phi^2 - \Delta\tau$	$-2 \cdot \Delta\phi - 2 \cdot \Delta\phi\Delta\tau$	
$P_{22.5} - P_{112.5}$			$\sqrt{2} \cdot (+0.5 + \Delta\phi - \Delta\phi^2 - 0.25 \cdot \Delta\tau^2)$
$P_{22.5} + P_{112.5}$	$+0.5 - 2 \cdot \Delta\phi\,(1 + \Delta\tau)$ $-0.5 \cdot \Delta\tau - \Delta\psi$	$+0.5 - 4 \cdot \Delta\phi^2 + 0.5 \cdot \Delta\tau + \Delta\psi$	
$P_{67.5} - P_{157.5}$			$\sqrt{2} \cdot (+0.5 - \Delta\phi - \Delta\phi^2 - 0.25 \cdot \Delta\tau^2)$
$P_{67.5} + P_{157.5}$	$+0.5 + 2 \cdot \Delta\phi\,(1 + \Delta\tau)$ $-0.5 \cdot \Delta\tau + \Delta\psi$	$-0.5 + 4 \cdot \Delta\phi^2 - 0.5 \cdot \Delta\tau + \Delta\psi$	

(56)

$$
\begin{cases}
(P_{22.5} - P_{112.5}) - (P_{67.5} - P_{157.5}) &= V \cdot 4\sqrt{2} \cdot \Delta\phi & (a)\\
(P_{22.5} - P_{112.5}) + (P_{67.5} - P_{157.5}) &= V \cdot 2\sqrt{2} \cdot (1 - 2 \cdot \Delta\phi^2 - 0.5 \cdot \Delta\tau^2) & (b)\\
(P_{22.5} + P_{112.5}) - (P_{67.5} + P_{157.5}) &= U \cdot 2\,(1 - 8 \cdot \Delta\phi^2 + \Delta\tau) + Q \cdot 4\,(-2 \cdot \Delta\phi\,(1 + \Delta\tau) - \Delta\psi) & (c)\\
(P_{22.5} + P_{112.5}) + (P_{67.5} + P_{157.5}) &= Q \cdot 2\,(1 - \Delta\tau) + U \cdot 4 \cdot \Delta\psi & (d).
\end{cases}
\tag{57}
$$

which leads to the combination of four angles of the quarter-wave retarder that can be used to determine all Stokes parameters QUV in four exposures (57). However, the simultaneous mode has two drawbacks. Firstly, it uses the sums of the differences $\sum d_k$ in (34) of the normalized intensities of the two polarized spectra (e.g. to derive Q) which makes it rather sensitive to any continuum errors in the polarized spectra (contrary to the differences where the continuum errors are mutually canceled out). Secondly, the polarization modulation function (28) with the angles separated by $45°$ has half reduced modulation amplitude in Q and U as compared with any other combinations of two measurements (e.g. $P_{45} - P_{135}$). In the following, we consider the statistical error budget for the simultaneous QUV mode.

4.3.1 Statistical error budget in simultaneous QUV mode

Suppose that the signal-to-noise ratio (S/N) of the two polarized spectra $R_\pm$ are equal. The S/N of the continuum normalized Stokes quv, as the inverse of the standard deviation in this case, obtained from two full- modulation polarization exposures, e.g. $(P_{45} - P_{135})$ for the quarter-wave or half-wave retarders, is $R_{quv} = 2 \cdot R_\pm$. For the half modulation amplitude (simultaneous mode) in (57), the S/N is $R_{qu} = \sqrt{2} \cdot R_\pm$ and $R_v = 2 \cdot R_\pm$.

To obtain all Stokes parameters quv in the separate mode, six exposures are needed in total to measure each of the Stokes parameters with two different angles of the polarimeter (V with the quarter-wave retarder, QU with the half-wave retarder or with no-retarder. The resulting S/N values R_{quv} for example are listed in the first row of the table below (58). In the simultaneous mode with only four exposures of the same or different duration, the S/N in V is always $\sqrt{2}$ larger than in QU as outlined in the last three rows of (58).

Exposure	$R_\pm$	R_v	R_{qu}
6×10 min	100	200	200
4×10 min	100	200	141
4×20 min	141	282	200
4×15 min	122	244	172

(58)

5 Polarimetric calibration

Any polarimetric calibration involves measurements of the two polarized-beam intensities in the spectrograph with respect to the angle of the polarization elements (e.g. retarder) as the response to the incident light of the known polarization state. The non-linear polarization modulation function (25) with a number of unknown parameters, i.e. angles of the polarization elements, is subsequently fit to the measured response function. The incident light of the known polarization state is typically produced with a continuum light source transmitted through a calibration element (a linear polarized or a retarder). Since the exact polarization state of the calibration element may not be exactly known at a given wavelength, its Stokes vector can be determined as a free parameter. For the continuum light source the total intensity in each polarized beams has to be accurately measured, which is affected by the transmission factors in the spectrograph as follows:

- Vignetting on the slit and/or fiber entrance due to imperfect adjustment or de-centering the polarized beams together with the chromatic shift of the beams due to dispersion of the polarizing beam-splitter, as well as angular or spatial precession of the beams (wobbling) due to rotation of the polarized elements.
- Difference in the transmission factors of the two fibers rendering the two polarized beams to the spectrograph. Furthermore, the difference may change with the temporal spatial orientation of the fibers and may have a hysteresis.
- Attenuation of the polarized light on the échelle grating depending on the orientation of the polarized ellipse with respected to the échelle grooves in case the two linearly polarized beams enter the spectrograph, or the fibers which have a polarization dispersion.

The intensity of the two polarized beams from the beam-splitter $I^\pm$, and these measured in the spectrograph $J^\pm$, are attenuated by the transmission parameters $f^\pm$ for each beam, so that

$$J^\pm = f^\pm \cdot I^\pm. \tag{59}$$

The *measured* relative difference of the polarized beams becomes

$$r = \frac{J^+ - J^-}{J^+ + J^-} = \frac{f + R}{1 + fR}, \tag{60}$$

where the relative difference of the beams and the relative transmission parameter in the spectrograph are

$$R = \frac{I^+ - I^-}{I^+ + I^-} \qquad \text{and} \qquad f = \frac{f^+ - f^-}{f^+ + f^-}. \tag{61}$$

The intensity of the light at the exit of the beam-splitter (23) is

$$I^\pm = A^\pm I \pm B^\pm P, \tag{62}$$

so that the relative difference of these two beams becomes

$$R = \frac{F_0 + p\,F}{1 + p\,F_1}, \tag{63}$$

where the intensity-normalized modulation function $p = P/I = qa_0 + ua_1 + va_2$ and

$$F_0 = \frac{A^+ - A^-}{A^+ + A^-},\ F_1 = \frac{B^+ - B^-}{A^+ + A^-},\ F = \frac{B^+ + B^-}{A^+ + A^-}.$$

In case of the Foster prism (40) we have $R = p \cdot (1 - L) - L$. In case of equal polarization transmission $A = A^\pm$ and $B = B^\pm$, we simply have

$R = p \cdot F$, so that for the latter case the measured relative difference of the two polarized beams

$$r = \frac{J^+ - J^-}{J^+ + J^-} = \frac{f + Fp}{1 + fFp}. \quad (64)$$

Since the polarization state of the calibration element may not be exactly known, it can be included as a free parameter to the polarization modulation function (25). By using (2) for the normalized Stokes vector, we can replace q, u, and v by the azimuthal angle χ and ellipticity β:

$$\begin{aligned} p = &(\cos 2\gamma \cos 2\phi + \sin 2\gamma \sin 2\phi \cos\tau) \cos 2\beta + \\ &\sin 2\phi \sin\tau \sin 2\beta, \end{aligned} \quad (65)$$

where $\gamma = \phi + \psi - \chi$. The relative difference (64) of the measured intensities

$$r(f, F, \psi, \Delta\phi + \phi', \tau, \chi, \beta; \phi') \quad (66)$$

is a function of the following unknown parameters: the relative transmissions in the spectrograph f and in the beam-splitter F, the beam-splitter orientation ψ, the retarder axis zero offset $\Delta\phi$ with respect to the beam-splitter axis, the retardation angle τ, and the azimuthal axis χ and ellipticity β of the polarization ellipse of the calibration element. The function is changing versus ϕ' as the actual position of the retarder. Most of the unknown parameters are dependent on wavelength.

Since some of the unknown parameters are correlated with each other, only a subset of parameters can be determined at one time depending on the configuration of the polarization elements. The nonlinear least-squares fit (Levenberg-Marquardt method, Press et al. 1992) of the relative difference function (64) to its measurements as a function of the retarder angle ϕ is used.

Some specific cases of the polarization elements configurations are outlined in the following:

- For unpolarized light with $q = u = v = p = 0$ as the calibration light, the relative difference function at any angle of the retarder is $r = f$. Ideally, it must be constant without showing any variations versus retarder angle.
- For the polarimeter configuration with no retarder $\tau = \phi = 0$ and the linearly polarized light $\beta = 0$ as the calibration light source, we have $p = \cos 2(\psi - \chi)$. Rotation of the calibration polarizer with the azimuthal angle χ allows to derive both transmission parameters f and F from the fit to the measured modulation function.
- For the circularly polarized calibration light source with $\beta = 45°$ and $\chi = 0$, and the polarimeter with the quarter-wave retarder in the beam, the modulation function is $p = \sin 2\phi \sin\tau$. The retarder angle $\phi = \Delta\phi + \phi'$ (unknown zero offset plus actual retarder orientation) and the retardation angle τ are fully correlated. Hence, this mode is not allowing to derive τ but only $\Delta\phi$ and f for the known τ. Also note the interplay between $\cos\tau$ and F in (65).
- For the linearly polarized calibration source ($\beta = 0$) and the polarimeter with the quarter and half-wave retarders in the beam allows to determine most of the unknown parameters: τ, $\Delta\phi$, and f. The modulation function reduces to $p = \cos 2\gamma \cos 2\phi + \sin 2\gamma \sin 2\phi \cos\tau$. Since the retarder angle ϕ is correlated with the azimuthal angle χ in γ, any misalignment offset in the polarization plane of the calibration source with respect to the beam-splitter optic axis results an erroneous offset of the retarder initial position $\Delta\phi$.
- The last unknown parameter is the azimuthal angle ψ of the polarization beam-splitter which cannot be calibrated internally with the polarization elements and has to be aligned externally by using two spatially separated polarized beams with respect to the great circle passing through the light source and the North celestial pole.

5.1 The use of polarimetric calibration

Once the polarimetric calibration parameters $\Delta\psi$, $\Delta\phi$, and $\Delta\tau$ are obtained as a function of wavelength, the next question would be how to use them for accurate reduction of the polarized stellar spectra in order to remove the cross-talk between Stokes parameters at each wavelength pixel.

Primarily, the polarimetric calibration is served in order to make a proper alignment of the polarization elements in the initial setup, specifically, the azimuthal angle of the whole polarimeter ψ with respect to the celestial pole, and the retarder optic axis orientation ϕ with respect to the optic axis of the polarizing beam-splitter.

In order to take into consideration all deviations of these angles (including retardation error $\Delta\tau$) during data reduction of polarized stellar spectra, one would need to solve a simple system of linear Eqs. (55) and (56) with respect to unknown Stokes Q, U, and V for each wavelength pixel. However, the main problem is that all these Stokes parameters must be measured quasi-simultaneously and with adequate signal-to-noise ratio in order to obtain the meaningful solution.

5.2 Polarimetric self-calibration reduction of spectra

Another practical solution is to fit the polarization modulation function (25) to the continuum normalized polarized spectra obtained at different angles of the quarter-wave retarder (57) in the simultaneous QUV mode. If all the calibration parameters are known in advance, the unknown Stokes parameters QUV can be easily obtained for each wavelength pixel from a linear least-squares fit to the polarized spectra.

The same applies to the half-wave retarder mode (55) with the angles separated by $90°$, e.g. $(P_0 + P_{90})$ and $(P_{22.5} + P_{112.5})$, where no terms with Stokes V are present and the cross-talk between Q and U is excluded with the known deviation of the retarder angle $\Delta\phi$ (by neglecting quadratic terms and $\Delta\psi$).

As the next step of further improvement and complication, the retarder optic axis orientation error, $\Delta\phi$, can be set as a free parameter with a slow variation versus wavelength. This requires a non-linear least-squares fit of the modulation function to the whole matrix of polarized spectra at different retarder angles for all wavelength pixels. This leads to a large block-diagonal design matrix with the first few rows occupied by the parametrization function elements of $\Delta\phi$ (e.g. coefficients of the Chebyshev polynomials). Given the large size of the resulting matrix of normal equations, the problem cannot be efficiently solved with the convenient Cholesky factorization in any reasonable computation time even after block-diagonal matrix storage and operational optimization. Hence, iterative methods must be used in this case, e.g. LSQR (Paige & Saunders 1982) which is based upon conjugate gradients method as applied to the least-squares problem.

The advantage of this approach is that it excludes from the fit the cross-talk between Stokes parameters induced by the retarder axis angle variations $\Delta\phi$ (see Sect. 7.2 for the results). The other calibration parameters $\Delta\tau$ and $\Delta\psi$ cannot be used as free parameters in the fit (as discussed in Sect. 5), because it requires the light to be linearly polarized.

6 Ratio of the polarized spectra

Semel et al. (1993) suggested a method which would eliminate the uncertainty introduced by the imperfect flat field correction for the CCD pixel-to-pixel noise. The method seems to be working perfectly for solar polarimetric observations (Bianda et al. 1998) and was extensively used for the extraction of stellar polarized spectra (Donati et al. 1999; Keller 2002, p. 340; Bagnulo et al. 2009). In the following we again reassess the accuracy of the method.

Let the function which describes the pixel-to-pixel sensitivity variations be denoted by $g^{\pm}$ for the area on the CCD occupied by the two polarized beams with the measured intensities $J^{\pm}$. The transmission parameters for the two polarized beams shall be $f_k^{\pm}$, where $k = 1, 2$ is the exposure number for the two angles of the polarization elements. Then

$$J_k^{\pm} = g^{\pm} f_k^{\pm} \cdot I_k^{\pm} = g^{\pm} f_k^{\pm} \cdot (A^{\pm} I \pm B^{\pm} P_k). \tag{67}$$

In order to spare unnecessary complications with the differential transmission factors of the beam-splitter, we set them equal $F = F^{\pm} = B^{\pm}/A^{\pm}$. Hence the ratio of the four polarized beams with the gain factors $g^{\pm}$ eliminated is

$$r = \frac{J_1^+}{J_1^-} \cdot \frac{J_2^-}{J_2^+} = f \cdot \frac{(1 - F^2 p_1 p_2) + F\,(p_1 - p_2)}{(1 - F^2 p_1 p_2) - F\,(p_1 - p_2)}, \tag{68}$$

where the relative transmission ratio for all four beams and the normalized Stokes parameters are

$$f = \frac{f_1^+}{f_1^-} \cdot \frac{f_2^-}{f_2^+} \qquad \text{and} \qquad p_k = \frac{P_k}{I}. \tag{69}$$

In general, the relative transmission f may have deviations from unity depending on the spectrograph setup, and the guiding and seeing condition between two exposures. Suppose that the relative ratio of the polarized beams is normalized to the smoothed curve fitted to f, i.e. $\tilde{r} = r/\tilde{f}$, so that we can replace r with $\tilde{r}$ and set $f = 1$.

The resulting un-reducible expression for the difference of the two normalized Stokes parameters is

$$p_1 - p_2 = \frac{1}{F} \cdot \frac{\tilde{r} - 1}{\tilde{r} + 1} \cdot (1 - F^2 p_1 p_2). \tag{70}$$

In case the amplitudes of the normalized Stokes parameter are small, $p_1 p_2 \ll 1$, and can be neglected, then the difference in the normalized modulation function is

$$p_1 - p_2 = \frac{1}{F} \cdot \frac{\tilde{r} - 1}{\tilde{r} + 1} \tag{71}$$

which gives an estimate of the respective Stokes parameter. An attempt to include higher orders of non-linear equation expansions (70) was made in Bianda et al. (1998). Naturally, for the amplitude of the signal, e.g. $v = p_1 = p_2 = 10\%$ the error $1/(1 - F^2 p_1 p_2)$ of the Stokes parameter estimate is about 1%. For smaller amplitudes it becomes indeed negligible.

7 Polarization performance of two instruments

In this section we show some practical implications of the polarimetric error propagation as described before. We use spectra of the same star obtained with two different instruments: the HARPS polarimeter (Snik et al. 2011; Piskunov et al. 2011) at the ESO 3.6 m telescope, and the SOFIN polarimeter at the 2.56 m NOT (described in the following section). The HARPS polarimeter consists of two exchangeable superachromatic PMMA quarter and half-wave retarders (Samoylov et al. 2004) on a rotary stage in front of the Foster prism fixed with respect to two entrance fibers of the spectrograph. The whole setup is located in the $F/8$ converging beam of the Cassegrain focus of the telescope.

7.1 The SOFIN spectropolarimeter

SOFIN is the high-resolution échelle spectrograph (Tuominen et al. 1999) mounted at the Cassegrain focus of the 2.56 m Nordic Optical Telescope (NOT). An optical camera with 1 m focal length provides the resolving power of about 80 000 with the entrance slit size of $0.5''$. Spectra are recorded on a Loral $2048 \times 2048 \times 15$ μm CCD which provides a limited wavelength coverage at the selected spectral range totaling in 24 double polarized orders having about 45 Å in length at 5500 Å.

The spectropolarimeter is a modified replica of the device described in Plachinda & Tarasova (1999). It consists of a rotating quarter-wave plate and a fixed polarization beam splitter situated in front of the entrance slit of the spectrograph in the converging $F/11$ beam from the telescope.

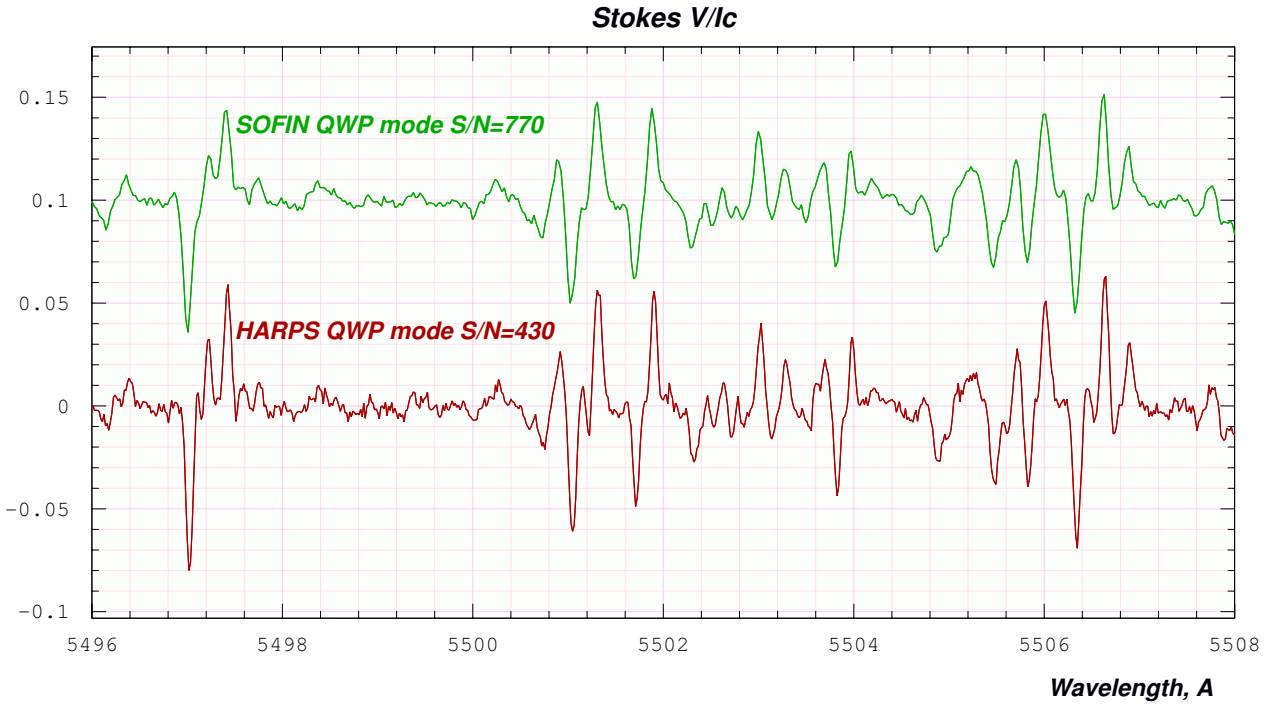

Fig. 4 (online colour at: www.an-journal.org) Comparison of the Stokes V/I_c for the Ap star γ Equ obtained with HARPS (lower panel) and SOFIN (upper panel).

The superachromatic (optimized for 4000–6800 Å) wave-plate of Pancharatnam design consists of five stretched PMMA acrylic films of half and quarter-wave zero-order retarders oriented at certain angles with respect to each other and laminated between two MgF_2 AR coated glass windows as described and manufactured by Samoylov et al. (2004). The retarder is situated on a rotary stage and turned by a stepper motor with a resolution of $15'$. The optic axis of the retarder is oriented by $45°$ with respect to the optic axis of the polarization beam splitter as the initial zero position. The retarder is rotating in the same direction as the azimuthal polarization axis is reckoned, i.e. clockwise in the direction of the light propagation (see Sect. 3).

The polarization beam splitter is a calcite plate with its entrance surface cut at $45°$ with respect to the optic axis of the uniaxial crystal providing a wavelength dependent double refraction of the two orthogonally polarized beams aligned along the entrance slit of the spectrograph. A custom made plate manufactured by B. Halle Nachfl. GmbH has an image separation of $4.6''$ at 5500 Å and provides sufficient separation of the doubled spectral orders up to 7000 Å. Since there is no aperture stop between two the polarized beams on the slit, the separation between orders is a trade-off between the seeing quality at the NOT and the number of spectral orders in one échelle image. A worse-than-average seeing may induce a polarization cross-talk between two partially overlapped polarized spectra in the red échelle orders.

Neither the retarder nor the calcite plate located in the converging $F/11$ beam produce any sensible detectable optical fringes in a wide range of échelle orders, which would be manifested as a linear trend of the interference frequency peaks versus spectral order number. In the original configuration with an additional quarter-wave plate after the beam splitter (to act as a depolarizer in order to minimize linearly polarized light attenuation on the échelle grating), the optical fringes were clearly detectable but were eliminated by a slight tilt of the polarimeter along the slit in cross-dispersion direction by half of the $F/11$ cone angle.

Before 2005 the polarimeter was used in a single beam mode due to insufficient spatial separation of the polarized beams, i.e. each of two polarized beams was exposured one after the other and their wavelength accuracy was based upon ThAr calibration made before and after each exposure. The new cross-dispersion prism installed in 2005 allows simultaneous registration of the two polarized beams in one exposure.

7.2 Polarimetric performance in comparison

The well-known rapidly oscillating, chemically peculiar (CP) star γ Equ (HD 201601, A9p, V=4.7) has a longitudinal magnetic field strength of around -1100 G (Hubrig et al. 2004) with a period over about 90 years (Leroy et al. 1994; Bychkov at al. 2006). Together with its slowest rotation among CP stars, $v \sin i \approx 10$ km/s, makes it a favorite object for any kind of polarimetric calibrations.

SOFIN spectra were obtained in August 2006, and HARPS spectra in July 2011. The Stokes V/I_c spectra are shown in Fig. 4 where the difference in the line depth are

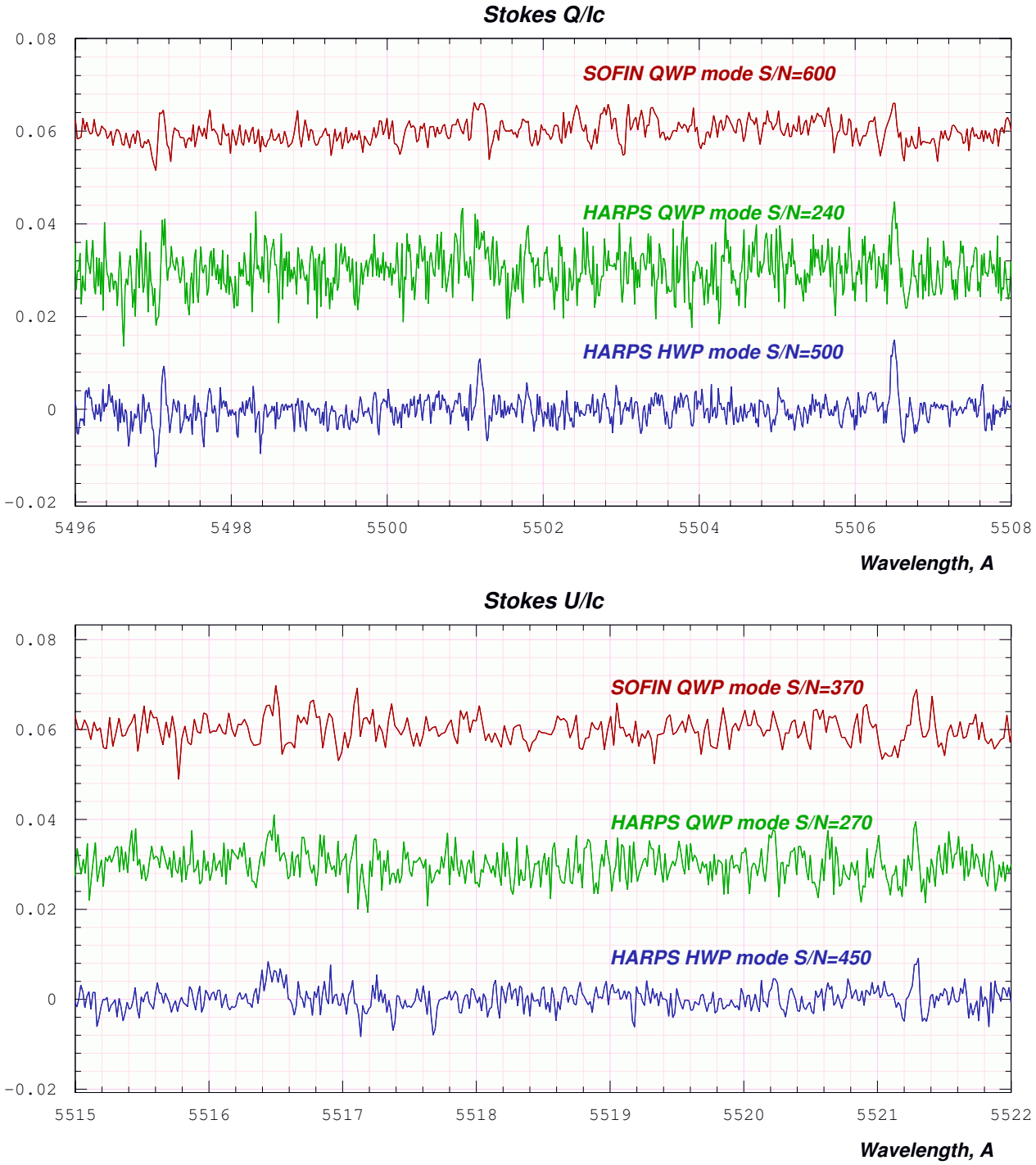

Fig. 5 (online colour at: www.an-journal.org) Comparison of the Stokes Q/I_c and U/I_c for the Ap star γ Equ obtained with HARPS in HWP and QWP modes (two lower spectra) and SOFIN in QWP mode (upper spectrum).

due to the difference in the spectral resolving powers for HARPS (110 000) and SOFIN (80 000). The difference in the signal-to-noise ratio is due to an about 50% higher throughput of SOFIN than HARPS after reduction to the same exposure time, resolving power, telescope size, zenith distance, and spectral region.

In Fig. 5, we demonstrate the application of the simultaneous QUV mode (Sect. 4.3.1) where the polarized Stokes QU and V spectra are obtained with the quarter-wave plate retarder (QWP). The linearly polarized QU spectra were subsequently obtained with HARPS with the half-wave plane retarder (HWP) for comparison. This comparison shows that the main features in QU are well reproduced in the QWP mode but a longer integration is needed to reach the same S/N as in the single HWP spectrum due to

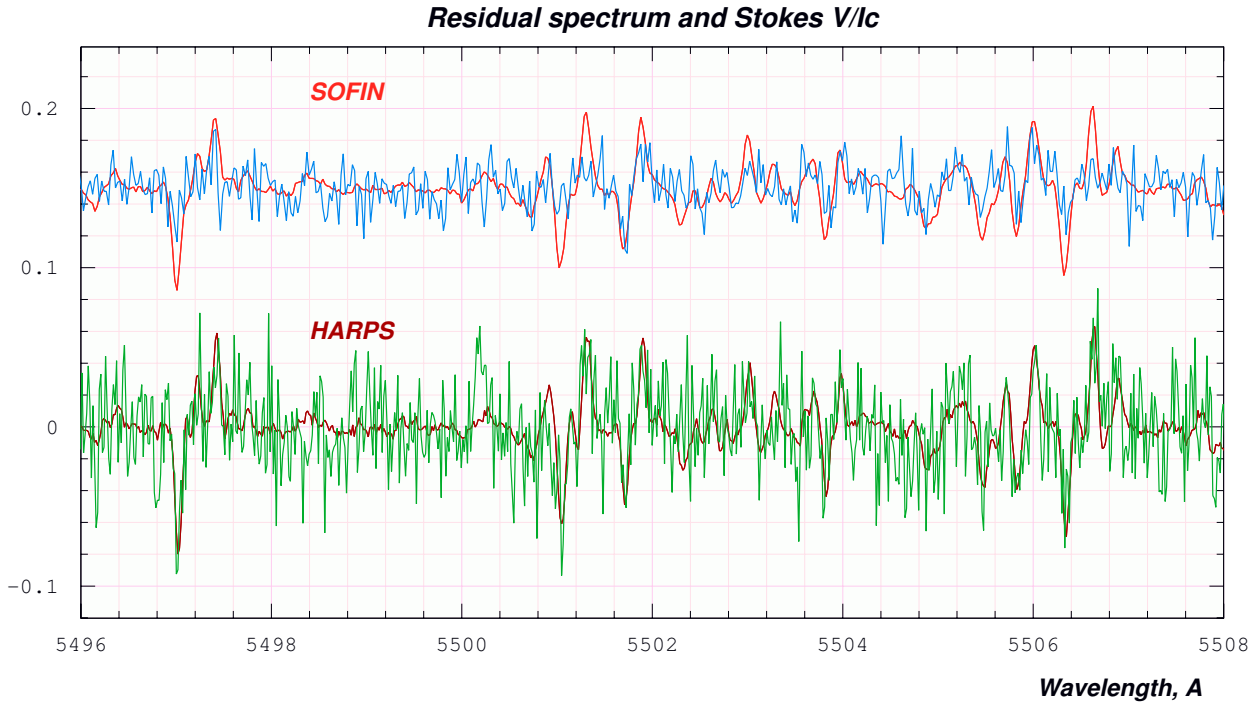

Fig. 6 (online colour at: www.an-journal.org) The residual spectra for HARPS (lower) and SOFIN (upper) overplotted with Stokes V/I_c. The residual spectrum $V/I_c \cdot \Delta\phi$ from (57a) is shown as the more noisy spectrum and scaled up 10 times in amplitude to match V/I_c.

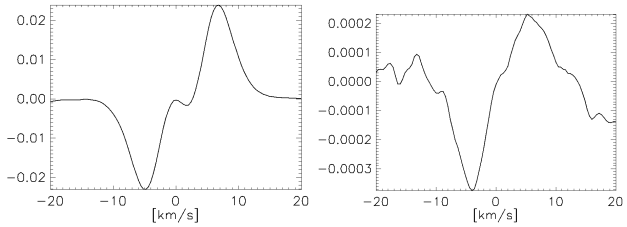

Fig. 7 The LSD profiles of Stokes V/I_c (left) and residual $V/I_c \cdot \Delta\tau$ (right) for HARPS obtained in HWP mode (55) with the retarder angle separated by $45°$. The LSD profile calculations are courtesy of T. Carroll (AIP).

the half amplitude in the polarization modulation function (Sect. 4.3.1).

The amplitude and its effect on the cross-talk between Q and U due to a wavelength dependent optic axis misalignment of the retarder $\Delta\phi$ is shown in Fig. 6. We used the QWP mode to derive the residual spectrum of $V/I_c \cdot \Delta\phi$ from (57a). The cross-talk term $\Delta\phi$ between Q and U is present in (57c) and (57d) in the QWP mode, as well as in almost every equation of (55) in the HWP mode.

The effect of the retardation error $\Delta\tau$ on the cross-talk is somewhat less pronounced and requires a higher signal-to-noise ratio to be seen. To do that, we computed LSD profiles (Donati et al. 1997) of the Stokes V/I_c and the residual spectrum $V/I_c \cdot \Delta\tau$ from HARPS spectra obtained in HWP mode with the retarder angles separated by $45°$: $(P_0 + P_{45})$ and $(P_{22.5} + P_{67.5})$ in (55) and shown in Fig. 7. The amplitude of the residual spectrum is about 1% of the Stokes V/I_c, which implies that $\Delta\tau$ averaged over a broad spectral range is about $0.5°$. This residual spectrum is co-added with the factor $1/2$ to Q/I_c or with $\sqrt{2}/2$ to U/I_c in all HWP mode combinations of angles, except the three combinations $(P_0 + P_{90})$, $(P_{45} + P_{135})$ and $(P_{22.5} - P_{67.5})$ in (55). In case of QU is 1% of V in amplitude, the cross-talk between QU and V is about 50%, i.e. up to one half of the amplitude in QU comes from V.

At the moment we were not able to detect any signature of the polarization interference (44) in HARPS spectra over a broad spectral range with the use of LSD profiles. Perhaps, this is due to a pickup-fence effect of the selected line list, moderate signal-to-noise ratio, and the broad modulation function L.

In Fig. 8, we show the global fit of the polarization modulation function (24) to the spectra obtained in the simultaneous QUV mode (57) with HARPS and SOFIN. The residual spectrum in Stokes U/I_c was formed as the difference between the global fits with and without inclusion of the retarder optic axis orientation ϕ as the free parameter. The residual spectra are scaled up seven times and plotted versus Stokes Q/I_c. The residual spectrum (with the factor two removed) consists of the term $Q/I_c \cdot 4\Delta\phi$ from (57c). The contribution of Q to U is in this example about 3.5%. The global fit of the SOFIN spectra with the retarder optic axis orientation ϕ included into the fit gives the same estimate for the angle as obtained from the polarimetric calibration in the same wavelength region.

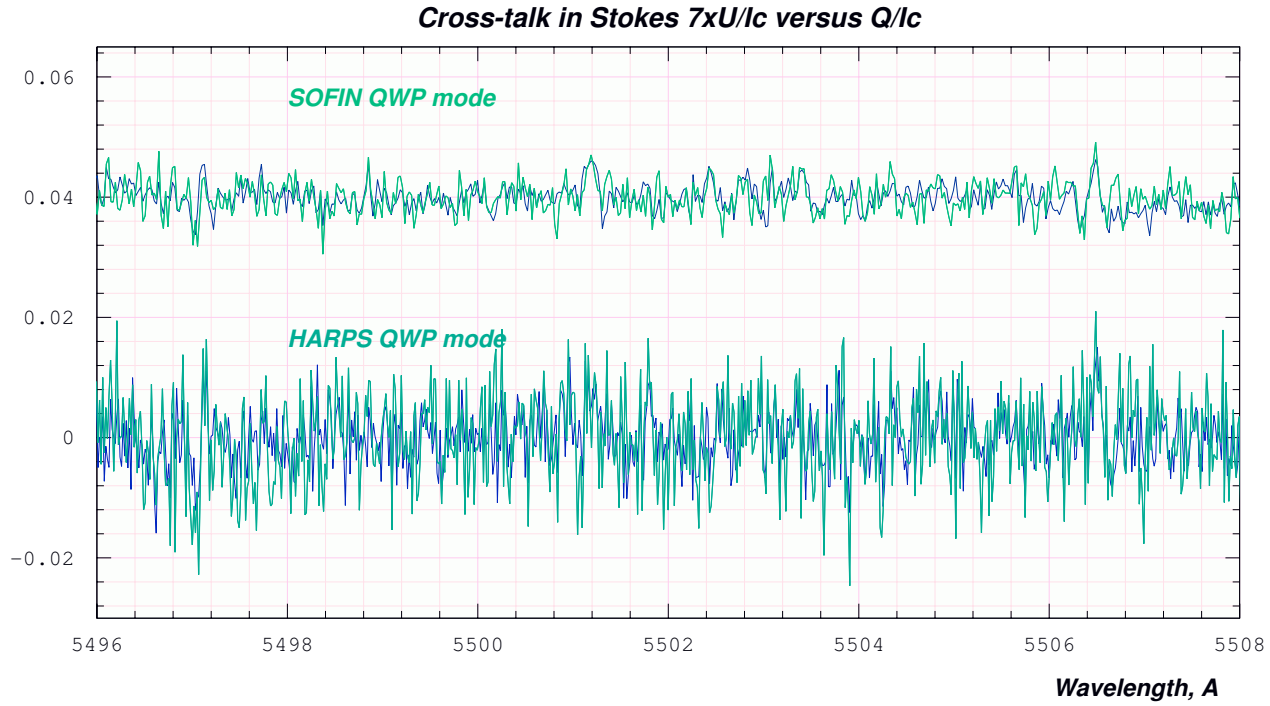

Fig. 8 (online colour at: www.an-journal.org) The residual spectra for HARPS (lower) and SOFIN (upper) overplotted with Stokes Q/I_c. The residual spectra, scaled seven times, are the differences between the two global fits of the polarization modulation function with the retarder optic axis orientation ϕ included or excluded from the fit. The spectra obtained in the simultaneous QUV mode with the quarter-wave retarder.

7.3 Conclusions

The aim of this work is to outline the optimal ways to minimize the cross-talk between Stokes parameters. We focus on stellar spectra obtained with a dual beam polarimeter with various configurations of the retarder element.

We showed in Sect. 4.3 that Stokes V can be obtained with the quarter-wave retarder with no cross-talk terms from Stokes QU and its accuracy limited only by the quadratic terms of the deviations of the polarization elements angles.

The optimal configuration to measure Stokes QU is described in Sect. 4.1 for a polarimeter with no retarder but the rotating polarizing beam-splitter fixed with respect to the entrance fibers (as laid out in Ilyin et al. 2011 for the PEPSI spectropolarimeter).

The polarimetric configuration with the half-wave retarder Sect. 4.2 can achieve high accuracy of the Stokes QU free of contribution from Stokes V for the retarder angles separated by 90° with a possible drawback of the continuum normalization uncertainties introduced to the Stokes spectra.

Finally, the simultaneous Stokes QUV mode with the use of the quarter-wave retarder advocated in Sect. 4.3 at (57), has the advantage of a homogeneous data set from which all Stokes parameters can be derived together with the wavelength dependent misalignment of the retarder optic axis. We employ a global non-linear fit of the polarization modulation function to the observed spectra at different angles of the retarder (Sect. 5.2). Some possible uncertainties of the continuum normalization for Stokes Q and half modulation amplitude for Stokes QU with respect to V are disadvantages of the method.

Acknowledgements. This paper includes data taken at the 2.56 m Nordic Optical Telescope (NOT), La Palma, Spain, and at 3.6 m Telescope, European Southern Observatory (ESO), La Silla, Chile. The PEPSI project was funded by the Science and Culture Ministry of the German State of Brandenburg (MWFK) and the German Federal Ministry for Education and Research (BMBF) and is supported by the German BMBF Verbundforschung through DESY grants 05AL2BA1/3 and 05A08BAC. The author thanks the referee of this paper for valuable discussions which helped to enlighten the manuscript, as well as to Dr. T.A. Carroll for his contribution on the LSD analysis.

References

Bagnulo, S., Landolfi, M., Landstreet, J.D., Landi Degl'Innocenti, E., Fossati, L., Sterzik, M.: 2009, PASP 121, 993
Bennett, J.M .: 1995, in: M. Bass, et al. (eds.), *Handbook of Optics II*, 2nd ed., Chapter 3
Bianda, M., Stenflo, J.O., Solanki, S.K.: 1998, A&A 337, 565
Born, M., Wolf, E.: 2002, *Principles of Optics*, 7th ed., Cambridge University Press, Cambridge
Bychkov, V.D., Bychkova, L.V., Madej, J.: 2006, MNRAS 365, 585
Carroll, T.A., Kopf, M., Ilyin, I., Strassmeier, K.G.: 2007, AN 328, 1043

Chandrasekhar, S.: 1950, *Radiative Transfer*, Oxford University Press, London
Clarke, D.: 2005, A&A 434, 377
Clarke, D.: 2010, *Stellar Polarimetry*, Wiley-VCH
Collett, E.: 1993, *Polarized Light: Fundamentals and Applications*, Marcel Dekker, New York
del Toro Iniesta, J.C.: 2005, *Introduction to Spectropolarimetry*, Cambridge University Press
Donati, J.-F., Brown, S.F.: 1997, A&A 326, 1135
Donati, J.-F., Semel, M., Carter, B.D., Rees, D.E., Collier Cameron, A.: 1997, MNRAS 291, 658
Donati, J.-F., Catala, C., Wade, G.A., Gallou, G., Delaigue, G., Rabou, P.: 1999, A&AS 134, 149
Donati, J.-F., Catala, C., Landstreet, J.D., Petit, P.: 2006, in: R. Casini, B.W. Lites (eds.), *Solar Polarization 4*, ASPC 358, p. 362
Eversberg, T., Moffat, A.F.J., Debruyne, M., et al.: 1998, PASP 110, 1356
Goodrich, R.W.: 1991, PASP 103, 1314
Halle Nachfl. GmbH: 2011, Product Catalog, www.b-halle.de
Hecht, E.: 2002, *Optics*, 4th ed., Addison-Wesley, San Francisco
Hubrig, S., Kurtz, D.W., Bagnulo, S., Szeifert, T., Schöller, M., Mathys, G., Dziembowski, W.A.: 2004, A&A 415, 661
Ilyin, I., Strassmeier, K.G., Woche, M., Dionies, F., Di Varano, I.: 2011, AN 332, 753
Keller, C.U.: 2002, in: J. Trujillo-Bueno, F. Moreno-Insertis, F. Sánchez (eds.), *Astrophysical Spectropolarimetry*, p. 303
Kochukhov, O., Piskunov, N.: 2008, in: K.G. Strassmeier, A. Kosovichev, J. Beckman (eds.), *Cosmic Magnetic Fields: From Planets, to Stars and Galaxies*, IAU Symp. 259, p. 653
Landi Degl'Innocenti, E., Landolfi, M.: 2004, *Polarization in Spectral Lines*, Kluwer Academic Publishers, Dordrecht
Leone, F., Bruno, P., Cali, A., et al.: 2003, in: S. Fineschi (ed.), *Polarimetry in Astronomy*, SPIE 4843, p. 465
Leroy, J.L., Bagnulo, S., Landolfi, M., Landi Degl'Innocenti, E.: 1994, A&A 284, 174
Mathys, G.: 1989, Fundamentals of Cosmic Physics 13, 143
Metz, K.: 1984, A&A 136, 175
Paige, C.C., Saunders, M.A.: 1982, ACM Trans. Math. Softw. 8, 43
Patat, F., Romaniello, M.: 2006, PASP 118, 146
Piskunov, N., Kochukhov, O.: 2002, A&A 381, 736
Piskunov, N., Snik, F., Dolgopolov, A., et al.: C.: 2011, Messenger 143, 7
Plachinda, S.I., Tarasova, T.N.: 1999, ApJ 514, 402
Press, W.H., Teukolsky, S.A., Vetterling, W.T., Flannery, B.P.: 1992, *Numerical Recipes*, 2nd ed., Cambridge University Press, Cambridge
Samoylov, A.V., Samoylov, V.S, Vidmachenko, A.P., Perekhod, A.V.: 2004, Journal of Quantitative Spectroscopy & Radiative Transfer 88, 319
Semel, M.: 2003, A&A 401, 1
Semel, M., Donati, J.-F., Rees, D.E.: 1993, A&A 278, 231
Snik, F., Kochukhov, O., Piskunov, N., et al.: 2011, in: J.R. Kuhn et al. (eds.), *Solar Polarization 6*, ASPC 437, p. 237
Strassmeier, K.G.: 2011, in: A. Bonnano, A. Kosovichev, E. Gouveia Dal Pino (eds.), *Advances in Plasma Astrophysics*, IAU Symp. 274, p. 274
Strassmeier, K.G., Woche, M., Ilyin, I., Popow, E., et al.: 2008, SPIE 7014, 21
Tuominen, I., Ilyin, I., Petrov, P.: 1999, in: H. Karttunen, V. Piirola (eds.), *Astrophysics with the NOT*, p. 47